Some simplifications to multianvil devices for high pressure experiments

D. Walker,* **M. A. Carpenter, C. M. Hitch**

Department of Earth Sciences, Downing Street, Cambridge CB2 3EQ, United Kingdom

Abstract

We describe a simplified multianvil system for high pressure and high temperature experiments based on the well-established octahedron-within-cubes geometry in use in many other laboratories. Departures in design from previous devices using this geometry include (1) use of a loose supporting ring that accommodates appreciable elastic strain under loading from within by an unanchored cylindrical cluster of removable tool steel wedges, (2) choice of height to diameter of the cylindrical cluster of wedges so that the negative cube geometry of the interior cavity that they surround does not have its angular relationships distorted under appreciable strain, (3) casting of composite gasket materials directly upon low porosity octahedral pressure media. The first two of these departures from established practices allow a drastic reduction in hardware cost, bulk, and production difficulty relative to current installations. The assembled multianvil module is cost effective, as well as being small and light enough to be inserted by hand in many of the standard hydraulic presses used for piston-cylinder work. The third departure reduces the risk of blowouts, of tedium, and of irreproducibility (during learning stages) of the normal procedure of cutting and attaching pyrophyllite gaskets. Using gaskets of Al_2O_3 in epoxy on a range of standard sizes of chrome magnesia octahedra, we are able to reproduce standard calibration point transitions with the same forces (and in some cases somewhat less force) required by other laboratories to achieve the same transitions with pyrophyllite gaskets. The overall performance of pressure, volume, and temperature (PVT) for this design is comparable to or better than extant octahedron-within-cubes devices. These developments should make multianvil experiments accessible to many existing piston-cylinder laboratories at modest incremental cost.

Introduction

Pressure is an important variable in mineralogical and petrological materials research. In condensed phases the high bulk modulus of the materials under investigation usually requires that pressures in the range of tens to hundreds of kilobars be applied in order for interesting property variations or phase transitions to occur. Practical devices producing static pressures at the upper end of this range are largely limited to diamond-anvil cells and a variety of multianvil devices. For large volume yields, development work has largely centered on the latter.

Multianvil devices were used in the 1950s in diamond synthesis work; for example, see von Platen (1962) and the summary in Hall (1960). Kawai and Endo (1970) used the octahedron-within-cubes geometry nested within a spherical seat pressurized by oil outside a rubber containment membrane. Split spherical or cylindrical seats, sometimes without the oil bag and sometimes with truncations to sectors of the seats, have been the basis of many subsequent versions of the nest for the octahedron-

within-cubes devices (e.g., Kumazawa et al., 1972; Ito et al., 1974; Akaogi and Akimoto, 1977; Yoneda et al., 1986; Takahashi, 1986; Ohtani et al., 1987). Ohtani (1987) has modified the nest for the anvils from a sphere to a long cylindrical cluster of wedges contained by a pair of separable, massive rings. The simplifications we describe are related to the previous design of Ohtani (1987), in that the wedges we use form a cylindrical cluster. However the wedges of the present design are loose and free to

$\longrightarrow$

Fig. 1. Plan and section drawings of the multianvil module. Uniaxial hydraulic press into which this module is positioned for axial loading is not shown. The plan view has been drawn with the top pressure distribution plate (G_1), the top three wedges (A_{4-6}), and the cubes plus the pressure medium assembly (C, D) removed. Critical dimensions listed as follows. (Gaps, their dimensions, and their filling materials are discussed in the text.) WEDGES. (A) AISI M2 tool steel hardened to R_c 62. Square face at 35°16' to axis of module; square face side 2.015 in. [5.118 cm]; lowest corner of square face 0.25 in. [6.35 mm] from basal surface; when 3 wedges assembled with gap of 1 mm between them, the cylindrical diameter is 7.990 in. [20.295 cm]; surface finish 8 micro inches or better. This high a hardness is unnecessary, and a subsequent version at R_c 58 has also performed well. Nevertheless, the continued use of M2 steel is recommended

PLAN VIEW
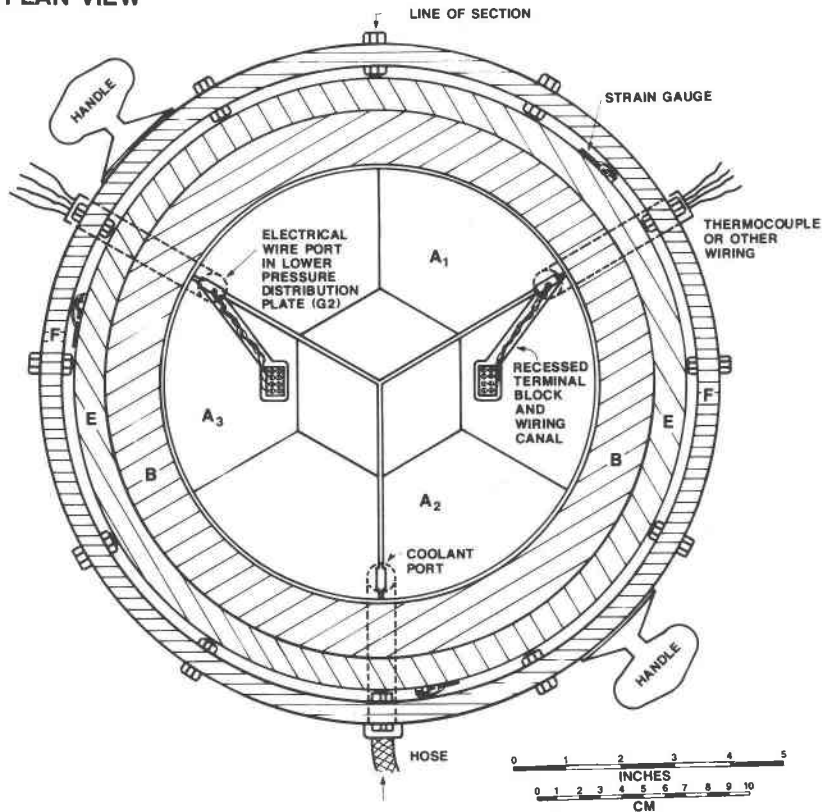
SECTION VIEW
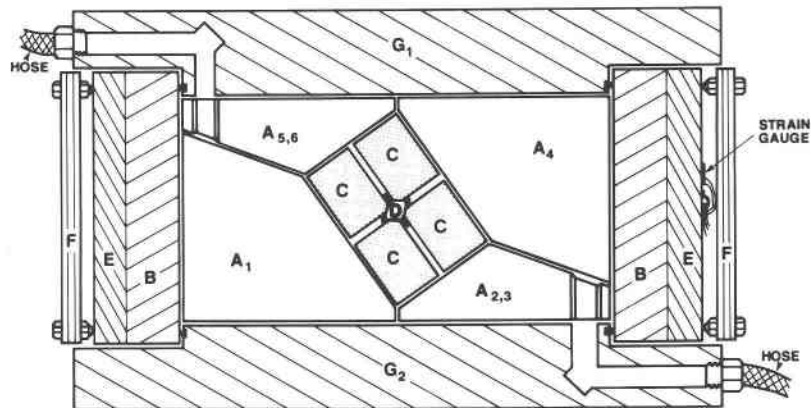
for its superior corrosion resistance. CONTAINMENT RING. (B) Stress ring of AISI H13 low-alloy tool steel hardened to R_c 49 and double tempered as supplied by Edward B. Williams Manufacturing Company, Foundry Lane, Smethwick, Warley, West Midlands B66 2LQ, United Kingdom. Nominal 0.2% proof stress is 14.5 kbar. O.D. 10.01 in. (25.425 cm), I.D. 8.000 in. (20.320 cm), length 5.0 in. (12.7 cm). Surface finish on bore better than 8 micro inches; 0.020 in. (0.51 mm) radius on all corners. ANVILS. (C) Tungsten-carbide cubes with corner truncations. Edge length 1.000 in. (25.40 mm); surface finish 8 micro inches or better. Hertel grade KMY (6% Co) used in testing. PRESSURE MEDIUM. (D) MgO with 5% Cr_2O_3 compressed to about 20% porosity; developed and supplied by Alan Hardstaff of G.R.–

Stein Refractories, Central Research Lab., Sandy Lane, Worksop, Nottinghamshire S80 3EU, United Kingdom. SAFETY RING. (E) Mild steel. 10.007 in. (25.4178 cm) I.D.; wall thickness 5/8 in. (16 mm); press fit onto ring B. SCATTER SHIELD. (F) Polycarbonate (Makrolon); 3.25 turns of a strip 3 mm thick and 5 in. (12.7 cm) wide rolled onto exterior of E and pinned to E with 2 dozen bolts. PRESSURE DISTRIBUTION PLATES. (G) Tool steel annealed AISI O1 hardened to R_c 18; 1.5 in. (3.8 cm) thick; 12 in. (30.5 cm) in diameter; raised "pillbox" of 7.80-in. (19.81-cm) diameter and 0.5-in. (1.27-cm) altitude forms an O-ring closure on bore of B. Tunnels and shafts bring coolant and wiring between wedges. (Al alloy used successfully in a subsequent version.)
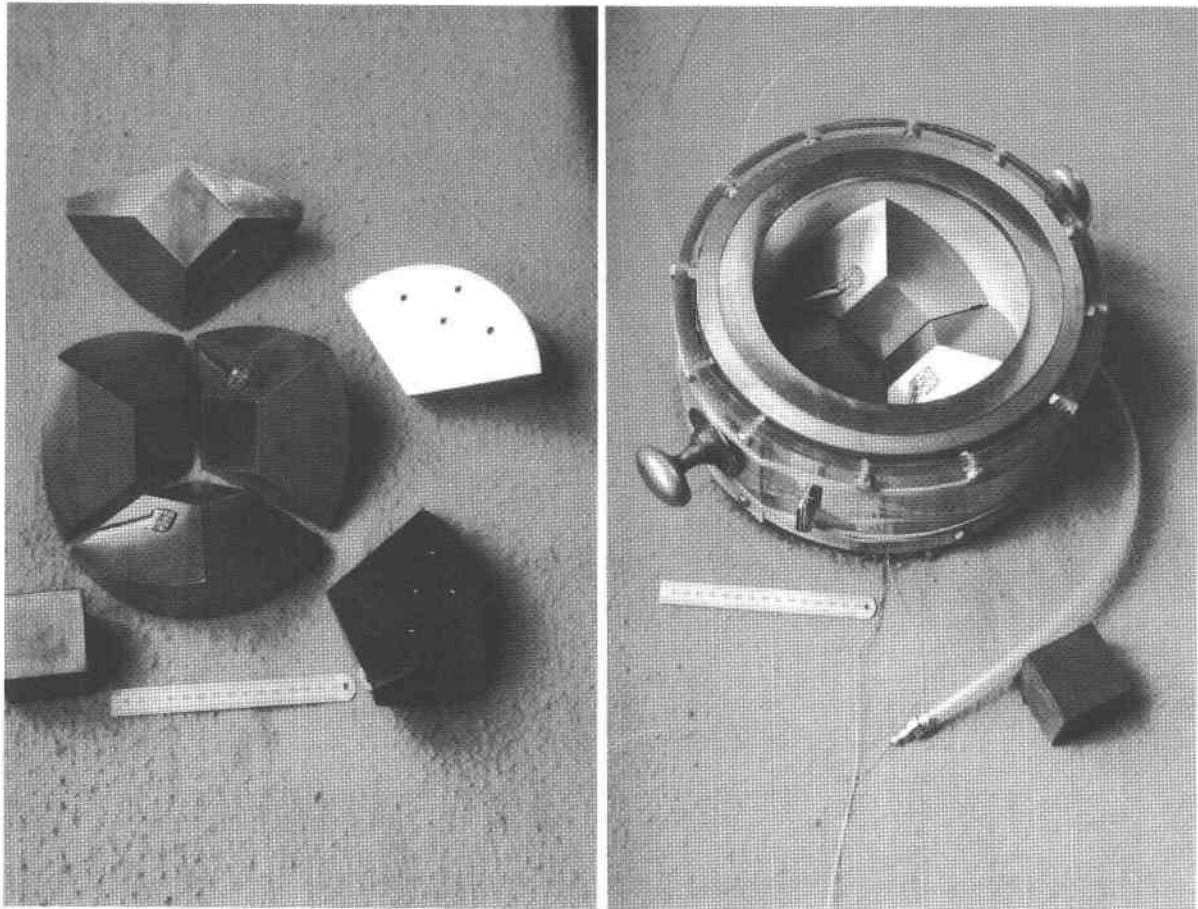
Fig. 2.   Photographs of the wedges and partially assembled module. Holes in the bases of the wedges are for dowel pins and bolt attachments used to promote uniformity in the fabrication of the wedges. Partially assembled view corresponds to the partially assembled plan view of Figure 1, except for the oblique view point.

float within the ring; and the wedge cluster's ratio of length to diameter is less than unity, rather than being a few times greater. Massive support of the cluster is not present, and substantial elastic strain of the supporting ring is induced during loading. Coolant is easily introduced between the components within the ring. Essentially we describe a soft-shell cylindrical nest for wedges which drive the standard octahedron-within-cubes payload. This modular device can be retrofitted into the hydraulic presses of many existing piston-cylinder laboratories.

EQUIPMENT DESCRIPTION

Plan and section drawings of the module are given in Figure 1. This module is inserted into a uniaxial hydraulic press to perform experiments. Uniaxial loading drives the lower set of wedges (A_{1-3}) toward the upper set of wedges (A_{4-6}) in the bore of the containment ring (B), forcing the tungsten carbide cubic anvils (C) to converge on the octahedral sample cavity (D). The containment ring (B) is jacketed by the safety ring (E) with a light press fit. Strain gauges are permanently mounted to the exterior

of the safety ring, which is surrounded by a polycarbonate scatter shield (F) with attached handles for manipulation of the ring and assembled module. Loading of the module is accomplished through pressure-distribution plates (G). Materials specifications and dimensions of these components are given in caption for Figure 1.

Several gaps exist between components. Between the carbide anvils (C) are gaskets, to be discussed in detail below. Between the anvils (C) and the wedges (A) are pads [0.020 in. (0.5 mm) thick] of glass-filled epoxy resin sheet (Tufnol grade 10G/40), which relieve any stress-causing irregularities on the interfaces between anvil and wedge, as well as accommodate the slip between anvil and wedge necessary for convergence during loading. Similar pads are in use in most multianvil laboratories. A gap 1 mm in plan view exists between the wedges (A), which is filled with Tufnol sheet 0.030 in. (0.76 mm) thick to position the wedges during module assembly. Between the wedges (A) and the pressure distribution plates (G) are disks 0.040 in. (1 mm) thick of Tufnol. These disks electrically isolate the wedges, absorb surface

irregularities, and accommodate the lateral motion of the wedges during loading [up to 0.010 in. (0.25 mm)]. Between the wedges (A) and the bore of the containment ring (B) is a gap of 0.005 in. (0.13 mm) filled with two sheets of polyester film. The outer sheet [0.003 in. (0.076 mm) thick] is coated on its interior glossy surface with polytetrafluorethylene (PTFE) spray (equivalent to Teflon). The inner sheet [0.002 in. (0.051 mm) thick] of polyester has its glossy side out to the PTFE-coated glossy side of the outer sheet. This configuration of lubricated interfaces between polyester sheets provides a slip surface to accommodate motion of the wedges (A) on the bore of the containment ring (B). The polyester sheets also provide electrical isolation of the ring from the wedges and absorb stress concentrations from surface flaws and debris on the bore of ring (B). The plastic sheets also isolate the bore of ring (B) from the mixture of soluble oil and water that circulates between the wedges (A) and between the cubes (C) as a coolant. Acetate sheets of the appropriate thickness have been found to work equally well, and the choice depends largely on ease of procurement.

Photos of the partially assembled module are shown in Figure 2. The weight of the module is low enough that a single small person can slide it into a hydraulic press without the aid of an air pad, lift, or rail system. In mass and ease of manipulation it is directly comparable to a standard Boyd and England (1960) assembled piston-cylinder stack. We have tested this module in a uniaxial press normally used for piston-cylinder work that could deliver about 500 tons of thrust from an 8-in. (20.32-cm) ram.

LOADING AND STRAIN TESTS

As uniaxial loading proceeds, the wedges converge on the cubic cavity and are consequently forced outward against the bore of the ring (B). The ring assembly swells as a result, and the wedges move radially as well as longitudinally along the module axis. The swelling of the ring under load was monitored directly with a movable dial indicator gauge and with permanently mounted strain gauges on the ring (E). No circumferential anisotropy of swelling can be detected at the outer surface of the ring once the assembly of interior wedges and cubes has been properly fabricated in terms of symmetry and uniformity of dimensions. In fact this lack of strain anisotropy of the ring makes it possible to test the correctness of the fabrication of the wedges and uniformity of the cubes. Dimensional imbalances of just a few 0.001 in. (0.025 mm) are easily detected by exterior strain anisotropies of the ring. A pair of typical plots of ring swelling on the outer diameter vs. hydraulic load is given in Figure 3. The plot in small open circles shows the swelling of the ring under load when only a single sheet of frosted polyester is used to lubricate the gap between the wedges (A) and the bore (B). The ring swelling is linear in applied load but shows substantial hysteresis during unloading. The ring binds the wedges, and they do not immediately slip back during
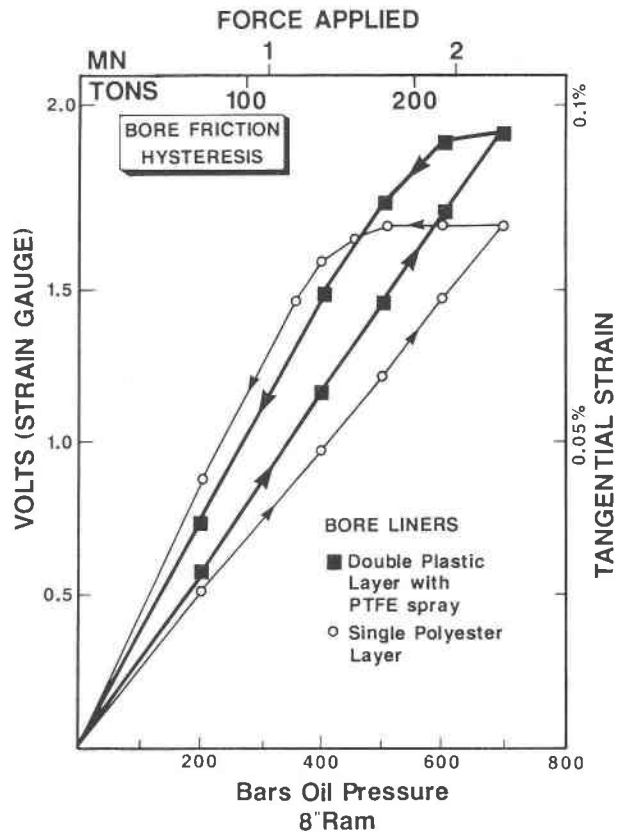

Fig. 3. Strain vs. load on press. Linear loading curves show markedly nonlinear unloading. Bore friction on the wedges is reduced through the expedient of providing a lubricated slip surface of plastic on plastic.

unloading. The extent of this hysteresis suggests that as much as 30% of the thrust may be dissipated into bore friction against the wedges. This is contrasted with the plot of large solid symbols for the double-lubricated film configuration generally used. Again the ring strain is linear in applied stress, but a substantially higher strain is realized for the same load. Furthermore, during unloading much less hysteresis is encountered. The extent of reduction of the width of the stress-strain loop suggests that bore friction has been reduced to the 10% of thrust level by the expedient of providing a lubricated slip surface of glossy plastic on glossy plastic. Many other lubrication combinations were tested, with none showing much better performance that the one described here, although several were considerably messier in practice. It is worth noting that PTFE is not the key ingredient here because a single 0.005-in. (0.127-mm) film of PTFE performed only marginally better that a single sheet of frosted polyester. Two dry sheets of glossy-to-glossy polyester performed better that either single sheet polyester or PTFE, so it appears that the plastic-to-plastic slip surface is the key ingredient, upon which further lubrication provides incremental improvement.

That frictional loss to the bore was the cause of the loading/unloading strain hysteresis was obliquely confirmed by measurement of ring strain along the axis of the module when internal loading proceeded only through the top pressure distribution plate. This could be accomplished by resting the lower end of the ring directly on the flange of the lower pressure-distribution plate and taking measurements with the dial indicator gauge up and down the outer ring surface. Strain measurements corresponding to the case of large hysteresis and poor lubrication in Figure 3 were about 20% higher in the top third of the ring than in the bottom third. In this configuration, only the top wedges were free to travel along the bore, and they sustain their frictional losses before stress is transmitted through the cubic anvils to the bottom set of three wedges. Thus the bottom three wedges push and swell the bottom of the ring to a lesser extent, determined by the bore friction. The hysteresis measurements of loading and unloading and the longitudinal anisotropy of strain measurements both suggest that the extent of thrust loss to bore friction is about 20–30% in the worst cases such as for the light symbols in Figure 3.

One might hesitate to think of the 10% frictional loss of the heavy symbols in Figure 3 as a best case. However when one considers how much of the total applied thrust is lost to gasket support rather than sample pressurization (roughly 50–90%, depending on the lab and gasket system), a 10% loss to friction is easier to tolerate. There is evidently much more potential scope for improving the efficiency of sample pressurization through attention to gasketing, where the major losses occur, than in removing the last small residual frictional losses. In light of the calibrations reported below, bore friction cannot be considered a major drawback to this design.

Nevertheless it should be possible to reduce this frictional loss still further in subsequent designs by splitting the single ring we have used into a pair of rings stacked on top of one another with compressible separators between. Rings capable of independent movement toward one another, each holding three wedges in place, will only encounter frictional losses at the tips of the wedges, which overlap the opposing ring. Splitting the ring into two has the added attraction that each ring is lighter and more easily manipulated. It also makes the inner cubic cavity more accessible for loading because the upper ring need not be fitted until the lower ring, lower wedges, and cubes are all fully assembled. A split ring also provides access for penetrating beam experiments (although there is no reason why suitable ports could not be introduced at the strategic places in a single ring). It is likely that future refinements in this design may proceed along these lines. A cautionary note about splitting the ring into two is that each ring must be proportionately larger that simply half of the single ring. This is because of the weaknesses associated with end stresses on the ring margins, where the two rings approach one another and support the wedge tips. The steel we have used in the device reported here

might need to have its wall thickened by as much as a factor of approximately 1.5 before it could be split into two rings and be expected to provide adequate support to the wedges.

A feature of some interest in Figure 3 is the extent to which the ring swells. At a load of 500 tons the ring diameter grows by almost 0.020 in. (0.51 mm). Clearly the wedges have a nontrivial radial displacement under load. The roughly comparable dimensions of wedge radius and height are a key feature in keeping the central cavity from distorting cubic angular relationships. An additional result of the extent of swelling of the ring under load is that the O-ring seals between the pressure distribution plates (G) and the ring bore (B) will no longer provide a seal. Thus it has proved handy to have a ready supply of rubber bands stretched onto the outside of the scatter shield (F). As the loading proceeds, these rubber bands can be dropped into the gap between the face of the pressure distribution plates (G) and the end of the ring (B) to form an end seal. Without this precaution, the circulating coolant will bathe the outside as well as the inside of the module, with untidy consequences. If safety concerns mandate reducing the exposure of the investigators to the apparatus under load, it will not be possible to decide in real time the number of rubber bands appropriate for the specific loading of the experiment. Alternate sealing procedures would need to be adopted. The use of O-ring seals on the end of the ring (B) is unlikely to be effective because of the close tolerances required for closure and the dynamic nature of the approach of the pressure distribution plate's (G) flange to the end of the ring (B) during an experiment. A more suitably compressible gasket material must be used to fill this gap before loading.

ALIGNMENT

The separated, unattached character of the wedges might be thought a design defect in terms of the difficulty in maintaining wedge alignment. In fact the reverse is true because the wedges are sufficiently lubricated and the geometric relations of the components are such that any unbalanced forces arising from misalignment are directed toward, and are capable of, nudging the wedges and cubes into proper alignment. The ability to self-align is critically dependent on the wedges being exactly symmetrical and the cubes being uniform in size. If this initial condition is satisfied, then the apparatus shows a remarkable capacity for self-organization. Even deliberate initial errors of up to 2 mm from center in the placement of Cu octahedra within the cubes produced highly symmetrical test pieces after closure of the jaws. The thickness of Cu fins extruded between the tungsten-carbide cube faces during jaw closure were uniform to within the ±0.05 mm (0.002 in.) measurable on a vernier caliper. The distance of extrusion of the fins was symmetrical enough that completed test pieces were in some demand as trinkets. Special initial or periodic alignment procedures to the wedges are unnecessary with this design.

CONTAINMENT RING DURABILITY AND SAFETY

The durability of the containment ring assembly under load is of some interest from the point of view of safety. Rough calculations using the nominal proof stress (14.5 kbar) suggest the ring would reach 0.2% strain at a uniaxial load approaching 700 tons. In point of fact this amount of strain was encountered at a uniaxial load of 500 tons, which also was the practical limit of the hydraulic system of the press used. The discrepancy between the designed and the observed strain may reflect some degradation of the nominal proof stress during the double tempering used to increase ring toughness, and it may reflect the crudeness of the calculations used. In any event, as long as the 0.2% strain limit is observed, an extended service life for the ring is anticipated. To ensure this limit is not exceeded, three strain gauges are attached to the exterior of the safety ring (E). Gauge voltages are monitored on a chart recorder along with other vital parameters of the experiment such as temperature, sample conductivity, and hydraulic system pressure, as indicated by a strain gauge attached to the outside of the ram.

Safety precautions taken against the unlikely event of ring failure include the safety ring (E) and the scatter shield (F). The mild steel of the same batch of tube stock used for the safety ring was certified to have passed a full flattening test without rupture. One measure of the danger associated with the failure of a pressure vessel is the quantity of elastic energy stored before rupture. Compound vessels of the Boyd and England (1960) type have at least as much energy stored as the energy of assembly of the two tapered rings and the insertion of the core. This is conservatively estimated at 10 kJ; any energy stored in sample pressurization increases the hazard. By contrast, an upper bound upon the elastic energy stored in this loaded multianvil module is provided by the product of the maximum force (500 tons) and the cube closure distance (2 mm). The elastic energy stored is undoubtedly very much less than this product because much of the work of closure is partitioned into anelastic deformation and extrusion of the gaskets, and an average force might be more appropriate to use than the maximum. Even so, this product is less than 10 kJ. Past experience with several catastrophic failures of compound pressure vessels of the Boyd and England (1960) design has shown mild steel to be effective as a safety ring. Because the safety ring (E) of the present design is at least three times more massive than the safety rings proved to have withstood catastrophic failures of more highly stressed compound vessels, we have felt reasonably confident in approaching this vessel under full load. Nevertheless it should be carefully noted that the use of inexpensive mild steel in this capacity is contrary to the best recommended practice, and that 300-series stainless steels are more ductile at high strain rates and may afford an extra margin of safety (Getting, 1979). Our extra margin of safety (not counting the rubber bands mentioned above) is the polycarbonate scatter shield (F).
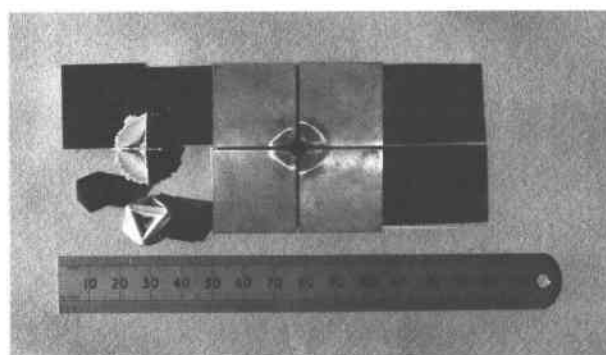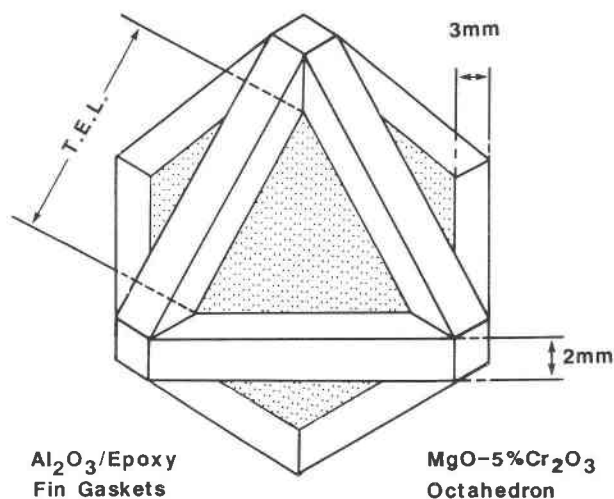

Fig. 4. (Top) Sketch of pressure medium with integrally cast gasketing fins. (Bottom) Photographs of actual examples of these combinations of pressure medium and gasket, as well as an example of a recovered experiment (ZnS transition) which was loaded to 200 kbar on 3-mm TEL tungsten-carbide anvils. The anvils are seen to have sustained appreciable plastic strain. The extrusion of the gaskets is satisfyingly uniform, and the gaskets clearly maintain their integrity even during unloading.

GASKETS AND PRESSURE MEDIA

Two innovations in gasketing and pressure media were employed. The first was to reduce to about 20% the porosity of the semisintered chrome magnesia (95% MgO and 5% Cr_2O_3) from which octahedra were sawed. Reduction of initial porosity is beneficial for pressure-generation efficiency because less compressive stroke is wasted in closing the initial porosity present. Chrome magnesia with only 20% porosity is quite easily machinable. Pure magnesia in this low initial porosity is slightly less easily machined, is a poorer insulator at very high temperature, and is a poorer pressure medium, as indicated by the study of force needed to recover fixed transition points, which is discussed below. Development work toward further densification of chrome magnesia is appropriate.

Our gasket system is illustrated in Figure 4. Fins that serve as gaskets during cube convergence are cast directly
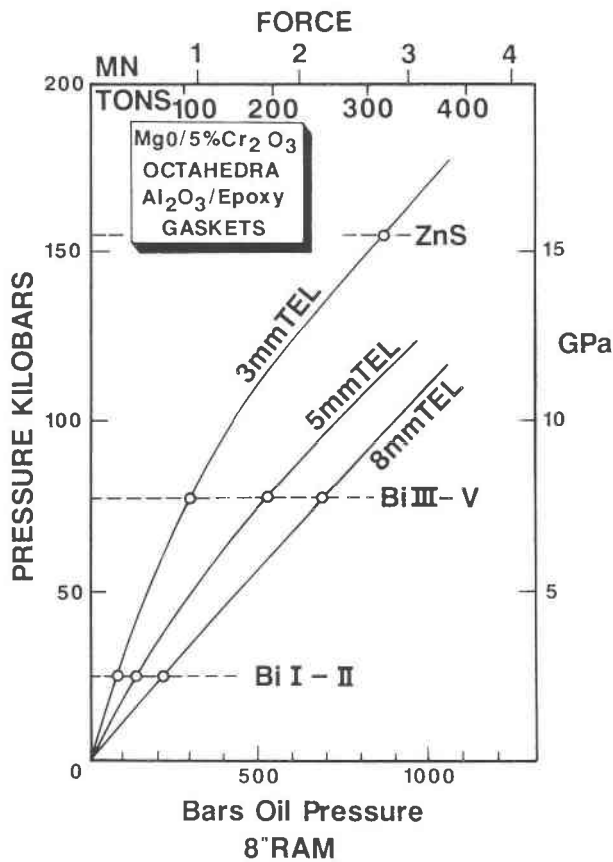
Fig. 5.   Fixed point calibrations for three sizes of anvil TEL for the low porosity (20%) chrome-magnesia pressure medium and integral gasket fins in standard use in this lab.
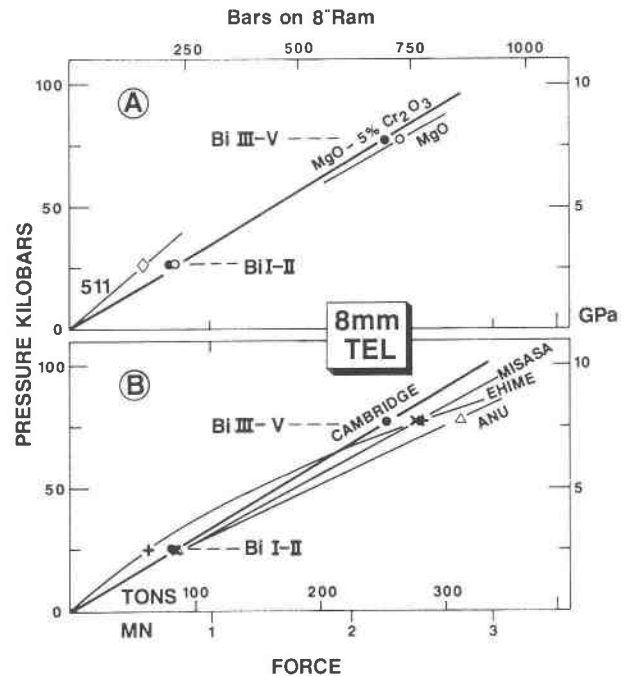

Fig. 6.   Calibrations for 8-mm TEL on Bi transitions. (A) Cambridge lab results for three ceramics. Chrome magnesia is slightly more efficient at translating thrust into sample pressure than chrome-free magnesia. Nonporous ceramics such as Aremco 511 are more efficient still, but suffer other problems discussed in the text. (B) Cambridge results for dense chrome magnesia with gaskets of epoxy and Al_2O_3 are compared to those for some other labs: Misasa (Takahashi, 1986), ANU (Ohtani et al., 1987), and Ehime (Ohtani, pers. comm.). Even with about 10% of thrust lost to bore friction, the use of dense, integrally gasketed pressure media in this lab gives an overall performance in the efficiency of converting thrust to sample pressure that is comparable to or better than currently acceptable standards. Thus bore friction is not a serious drawback to this multianvil nest design. Adoption of denser pressure media and these gasketing procedures could improve the performance of friction-free devices.

on the edges of the octahedra. We have experimented with several materials, the most successful to date being a composite of Al_2O_3 (a gritty powder supplied by BDH under the name calcined alumina) bonded by epoxy resin (Buehler Epoxide) in a ratio of 2:1 by weight. The composite is prepared by mixing powder with premixed resin and hardener. The material for pressing into the molds should be very sparingly wetted with the epoxy. A good measure of the richness of mixture desired is that the mix should wad and cling to a wooden spatula without looking at all wet. PTFE cubes with truncations to simulate tungsten-carbide anvils are spaced apart with PTFE sheet of the desired fin thickness (2 mm in all cases). The chrome-magnesia octahedron is placed in the segmented mold, and the composite is squashed into the spaces to become fins after curing. Figure 4 contains a photograph of the finished product, which can then be drilled or cut for heater insertion, wiring connections, and so forth. This procedure ensures a minimum of initial space due to the mismatch of gasket and MgO, reduces the chances of gasket misplacement, and replaces the tedium of cutting and pasting pyrophyllite with the tedium of cleaning up after epoxy dribbles.

This gasket composite is much less brittle than pyro-

phyllite and forms an extremely robust stockwork around the pressure medium. We suspect that the toughness of these integral gaskets, in addition to the self-alignment capacity of the wedges, plays a role in the low incidence of blowouts experienced in this lab—one in six months, which occurred at only 25 kbar through the ill-considered inclusion of polyester in the pressure medium. The performance of this composite material as a high pressure gasket may be judged objectively from the calibrations reported in the next section.

CALIBRATIONS

Three standard electrical resistance-drop transitions are shown in Figure 5 as a function of ram oil pressure and equivalent tons of force of uniaxial loading: Bi I-II at 25.5 kbar, Bi III-V at 77 kbar, and ZnS at 155 kbar (Lloyd, 1971; Piermarini and Block, 1975). Three sizes of anvil

truncation were tested: truncated edge lengths (TEL) of 8, 5, and 3 mm, which correspond to octahedral pressure media of initial edge dimensions 14, 11, and 8.5 mm. In all cases gaskets were 2 mm thick and extended 3 mm from their line of exterior intersection with the surface of the octahedron (which is always chrome magnesia in Fig. 5). A regular behavior is obvious. Furthermore, this plot highlights the fact that pressures in the normal range of other octahedron-within-cubes devices can be achieved by this design. We have successfully loaded 3-mm truncations to about 200 kbar without blowout or other equipment failure. Figure 4 shows a sample assembly and its gaskets recovered from one such experiment.

Comparison of our 8-mm TEL results for chrome magnesia is made to results for chrome-free magnesia in Figure 6A. It is clear that chrome magnesia is a slightly better pressure medium. An even higher efficiency of conversion of thrust into sample pressure was experienced using a nonporous, castable ceramic made of MgO and zirconia (Aremco 511). Only about 75% of the forced needed to achieve the Bi I-II transition with the other materials was required in this case. Unfortunately this material is not fully suitable for other reasons. Its mechanical nonuniformity promoted fin disintegration shortly after passing the transition from Bi II to Bi III. Nevertheless this result does indicate the benefits to be realized by reducing pressure medium porosity.

Figure 6B contains comparative results from other labs reporting Bi calibrations at 8-mm TEL. Our results are quite comparable to, or in some cases somewhat better than, those of the other labs in terms of the efficiency in converting thrust into sample pressure. Clearly this minimalist design does not sacrifice performance for simplicity of apparatus construction or ease of gasket preparation. In this context, anxiety over bore friction in the present design would seem to be misplaced. An obvious corollary is that other labs enjoying equipment free of bore friction might be able to improve their performance by adopting these gasketing procedures with lower porosity pressure media.

In other respects, such as heating, the performance of this design is also comparable to extant equipment. We have been able to pass the Mo melting point at 100 kbar on 8-mm TEL assemblies. Exactly the same strengths and weaknesses of all multianvil heating systems are shared by this one. However, the present design offers one advantage in that it is easy to circulate coolant within the sealed ring to keep the pads between the anvils and wedges from softening when hot and to keep the tungsten-carbide cubes cool. When coolant circulates, we have determined the temperature at the 8-mm TEL anvil tips to be about 250 °C, when the hot spot of a tube furnace with a diameter of 3.4 mm is in excess of 2000 °C at 100 kbar within 14-mm chrome magnesia octahedra. Without the coolant, the outer surfaces of the anvils approach this temperature in the steady state even when the interior sample temperature only approaches 1000 °C. Cooling the carbide should improve its performance.

CONCLUSIONS

A simple design is presented that duplicates the *PVT* performance of larger, standard octahedron-within-cubes multianvil devices. The device could be retrofitted into many existing piston-cylinder laboratories to enable research to 200+ kbar to be performed more widely.

REFERENCES CITED

Akaogi, M., and Akimoto, S. (1977) Pyroxene-garnet solid-solution equilibria in the systems $Mg_4Si_4O_{12}-Mg_3Al_2Si_3O_{12}$ and $Fe_4Si_4O_{12}-Fe_3Al_2Si_3O_{12}$ at high pressures and temperatures. Physics of the Earth Planetary Interiors, 15, 90–106.

Boyd, F.R., and England, J.L. (1960) Apparatus for phase equilibrium measurements up to 50 kilobars and temperatures to 1750°C. Journal of Geophysical Research, 65, 741–748.

Getting, I.C. (1979) Lubrication and safety in compound pressure vessels. In K.D. Timmerhaus and M.S. Barber, Eds., High pressure science and technology, vol. 1, p. 835–845. Plenum, New York.

Hall, H.T. (1960) High pressure methods. In High temperature technology, p. 145–156, 335–336. McGraw-Hill, New York.

Ito, E., Matsumoto, T., and Kawai, N. (1974) High-pressure decompositions in manganese silicates and their geophysical implications. Physics of the Earth Planetary Interiors, 8, 241–245.

Kawai, N., and Endo, S. (1970) The generation of ultrahigh hydrostatic pressure by a split sphere apparatus. Reviews of Scientific Instruments, 41, 425–428.

Kumazawa, M., Masaki, K., Sawamoto, H., and Kato, M. (1972) Guide blocks and compressible pads for the practical operation of multi-anvil sliding system for the production of high pressure. High Temperature–High Pressure, 4, 293–310.

Lloyd, E.C. (1971) Editorial introduction and summary to: Accurate characterization of the high-pressure environment. U.S. National Bureau Standards Special Publication, 326, 1–3.

Ohtani, E. (1987) Abstract from the Kobe High Pressure Conference.

Ohtani, E., Irifune, T., Hibberson, W.O., and Ringwood, A.E. (1987) Modified split-sphere guide block for practical operation of a multianvil apparatus. High Temperature–High Pressure, 19, 523–529.

Piermarini, G.J., and Block, S. (1975) Ultra high pressure diamond-anvil cell and several semiconductor phase transition pressures in relation to fixed point pressure scale. Reviews of Scientific Instruments, 46, 973–980.

Takahashi, E. (1986) Melting of a dry peridotite KLB-1 up to 14 GPa: Implications on the origin of peridotitic upper mantle. Journal of Geophysical Research, 91, 9367–9382.

von Platen, B. (1962) A multiple piston, high pressure, high temperature apparatus. In R.H. Wentorf, Ed., Modern very high pressure techniques, p. 118–136. Butterworths, Washington, DC.

Yoneda, A., Kato, M., Kozuki, Y., Sawamoto, H., Kumazawa, M., and Makino, R. (1986) The use of sandwich-type composite metal gaskets in an MA8 type apparatus to generate 15 GPa in a 1.8 cm³ sample volume. High Temperature–High Pressure, 18, 301–310.